Communication

Binary hole transport materials blending to linearly tune HOMO level for high efficiency and stable perovskite solar cells

Xinxing Yin[a], Changlei Wang[b], Dewei Zhao[b], Niraj Shrestha[b], Corey R. Grice[b], Lei Guan[b], Zhaoning Song[b], Cong Chen[b], Chongwen Li[b], Guoli Chi[a,b], Baojing Zhou[a,b], Jiangsheng Yu[a], Zhuohan Zhang[a], Randy J. Ellingson[b], Jie Zhou[a,*], Yanfa Yan[b,*], Weihua Tang[a,*]

[a] *Key Laboratory of Soft Chemistry and Functional Materials (Ministry of Education of China), Nanjing University of Science and Technology, Nanjing 210094, China*
[b] *Department of Physics and Astronomy and Wright Center for Photovoltaics Innovation and Commercialization, The University of Toledo, Toledo, OH 43606, United States*

A B S T R A C T

To maximize the photovoltaic performance of perovskite solar cells (PVSCs) by developing new hole-transport layer (HTL) materials, the precise tuning of their energy levels especially the highest occupied molecular orbital (HOMO) is highly desirable. Here, a simple binary strategy for the first time is proposed to acquire ideal HOMO level by optimizing the composition of binary blend HTLs including CZ-TA (HOMO = −5.170 eV) and CZ-STA (HOMO = −5.333 eV). By adding 10 wt% CZ-STA, the binary HTM (HOMO = −5.199 eV) based perovskite solar cells achieve a maximum power conversion efficiency of 19.85% (18.32% for CZ-TA). The introducing of S atom in CZ-STA not only downshifts HOMO level but also forms stronger Pb-S interaction with perovskites than Pb-O in CZ-TA, leading to better device performance and reduced hysteresis. Importantly, the un-encapsulated PVSCs using CZ-TA:CZ-STA (90:10, w/w) binary HTL exhibit good environment stability in ambient air, maintaining over 82% of their initial efficiency after 60 days' storage with a relative humidity around 50%. Therefore, this strategy provides new insights on HTL development to push forward the progress of the emerging PVSCs

1. Introduction

In the past few years, organic-inorganic hybrid perovskite solar cells (PVSCs) have witnessed a rapid development due to their facile solution fabrication, strong light absorption over a broad spectrum, long carrier lifetime and diffusion length [1–5]. The certified power conversion efficiency (PCE) has reached 22.7% from the initial 3.8% [6–10]. In a typical PVSC device, electron transport layers (ETLs, *n*-type semiconductors) and hole transport layers (HTLs, *p*-type semiconductors) are usually required to assist charge separation and transport [11–14]. State-of-the-art high-performance PVSCs commonly use organic materials especially 2,2′,7,7′-tetrakis(*N,N*-di-*p*-methoxyphenylamino)-9,9′-spirobifluorene (spiro-OMeTAD) as HTL [15–18]. However, the complex multi-step synthesis and expensive sublimation process greatly limit its commercial application. Moreover, spiro-OMeTAD needs to be exposed to ambient environment for a long-time oxidation process to reach peak PCE. This is also a great drawback for industrial use.

Considering the disadvantages mentioned above, many efforts have been made by researchers all over the world to replace spiro-OMeTAD

[9,19–24]. Malinauskas et al. [21] developed an effective HTL material named V862 through two-step reaction and the PCE can reach 19.96% with a total cost of only 23.11 \$ g^{-1} (∼ 500 \$ g^{-1} for spiro-OMeTAD). By simply replacing spiro core with fluorene–dithiophene, Saliba et al. [25] synthesized FDT and PVSCs with this HTL showed an impressive PCE of 20.2%. Meanwhile, the lab synthesis costs of FDT is only one fifth of spiro-OMeTAD. Hou et al. [9] adopted Ta-WOx modified PDCBT to reduce V_{OC} losses and acquired a PCE as high as 21.2%. Recently, we reported a simple carbazole-based HTL, CZ-TA, synthesized through a facile one-step reaction with improved hole transport and reduced cost (1/80 of spiro-OMeTAD) [26,27]. PVSCs using CZ-TA as HTL showed a PCE of 18.32% with an impressive fill factor (FF) over 81% and good device stability. Additionally, CZ-TA does not require oxygen doping, eliminating the potential drop of PCE upon device encapsulation. The main drawback of CZ-TA is the relatively low V_{OC} (1.044 V), indicating the mismatch of energy level [28]. It is well known that appropriate energy-level alignment can facilitate charge extraction and transport, leading to improved V_{oc} J_{sc} and FF. However, in many cases, although careful theoretical simulation and calculation have been carried out

---
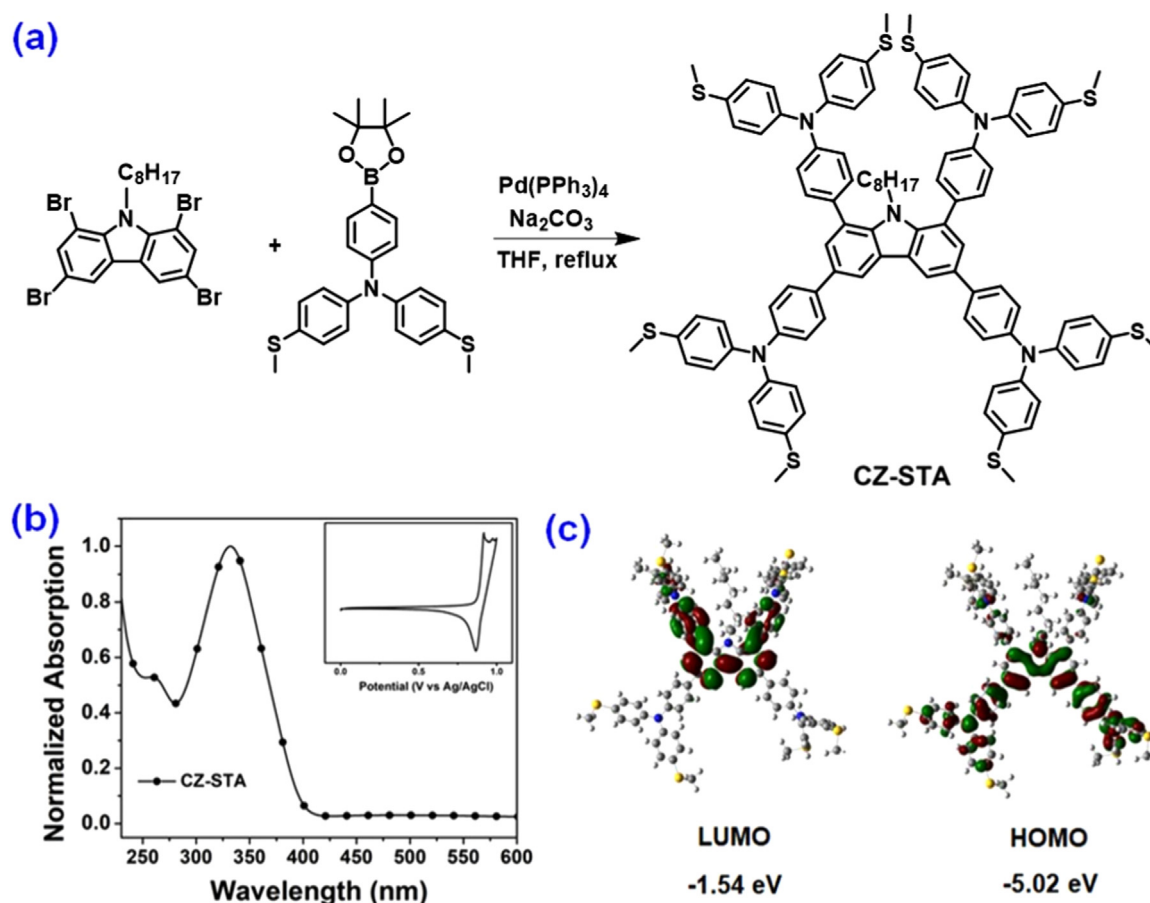
Fig. 1. (a) Synthetic route for CZ-STA. (b) Absorption spectra of CZ-STA film, the inset is cyclic voltagram of CZ-STA in 0.1 mol L^{-1} n-Bu$_4$NPF$_6$ solution in acetonitrile. (c) DFT-calculated HOMO and LUMO electronic structures of CZ-STA.

during HTL molecular design, the actual highest occupied molecular orbital (HOMO) level of HTL may still not be at ideal position resulting in V_{oc} loss [19]. Thus, simple, precise and efficient tuning of HOMO level is necessary for maximizing device performance when developing new HTL materials.

Herein, we report a new strategy for linearly tuning HOMO level of HTL materials to obtain maximum device performance. With CZ-TA as an example, firstly, we have designed and synthesized 4,4',4'',4'''-(9-octylcarbazole-1,3,6,8-tetrayl)tetrakis(*N,N*-bis(4-methylthiophenyl)aniline) (CZ-STA). By replacing methoxy group on CZ-TA with methylsulfanyl group, CZ-STA exhibits a deeper HOMO level due to the π-acceptor capability of sulfur atom. It can form $p\pi$(C)–$d\pi$(S) orbital overlap where divalent sulfur accepts π-electron from the π-orbital of C=C bonds into its empty 3d-orbitals [29,30]. Besides, stronger Pb-S interaction will also lead to more efficient charge extraction and surface traps passivation [31]. With CZ-STA in hand, HOMO levels can be easily tuned by changing ratios of CZ-TA and CZ-STA. Since these two molecules have almost the same conjugated structure, they are preferred to form very compatible blends [32,33]. Meanwhile, the S atoms of CZ-STA and O atoms of CZ-TA may form S…O non-covalent interactions in solid state to enhance their packing in HTL layers [34]. PVSCs using CZ-TA: CZ-STA (90:10, weight ratio) as HTL have reached a champion PCE of 19.85% (18.32% for CZ-TA) under reverse voltage scan and a steady-state efficiency of 19.55% (16.36% for CZ-TA). Compared with pure CZ-

TA (V_{OC} = 1.044 V, J_{SC} = 21.66 mA cm^{-2}, FF = 81.0%), binary blend HTL system showed increased V_{OC} and J_{SC} without sacrificing FF (V_{OC} = 1.082 V, J_{SC} = 22.51 mA cm^{-2}, FF = 81.5%). Moreover, the cost for lab synthesis and purification of both CZ-TA (~ \$25/g) and CZ-STA (~ \$32/g) is much lower than that for spiro-OMeTAD (see cost calculation in Supporting information). It's worth noting that the CZ-TA:CZ-STA (90:10) blend HTL based devices can maintain over 82% of its initial PCE after storing for 60 days in air with a relative humidity around 50% without encapsulation. To the best of our knowledge, this is the first report of precisely tuning HTL energy level through a simple and cost-effective binary blend strategy.

2. Results and discussion

The synthetic route of CZ-STA is outlined in Fig. 1a and detailed synthesis can be found in Supporting information (SI). 1,3,6,8-Tetrabromo-9-octylcarbazole was obtained following the same procedure in our earlier report [26]. The details of synthesis of 4-methylthio-N-(4-methylthiophenyl)-*N*-(4-(4,4,5,5-tetramethyl-1,3,2-dioxaborolan-2-yl)phenyl)aniline are outlined in SI [31,35]. After that, Pd-catalyzed Suzuki reaction was carried out to produce final CZ-STA with 78% yield. Simple column chromatography purification was adopted to acquire analytically pure CZ-STA for PVSC application, directly avoiding expensive sublimation process. The chemical structure of CZ-STA was
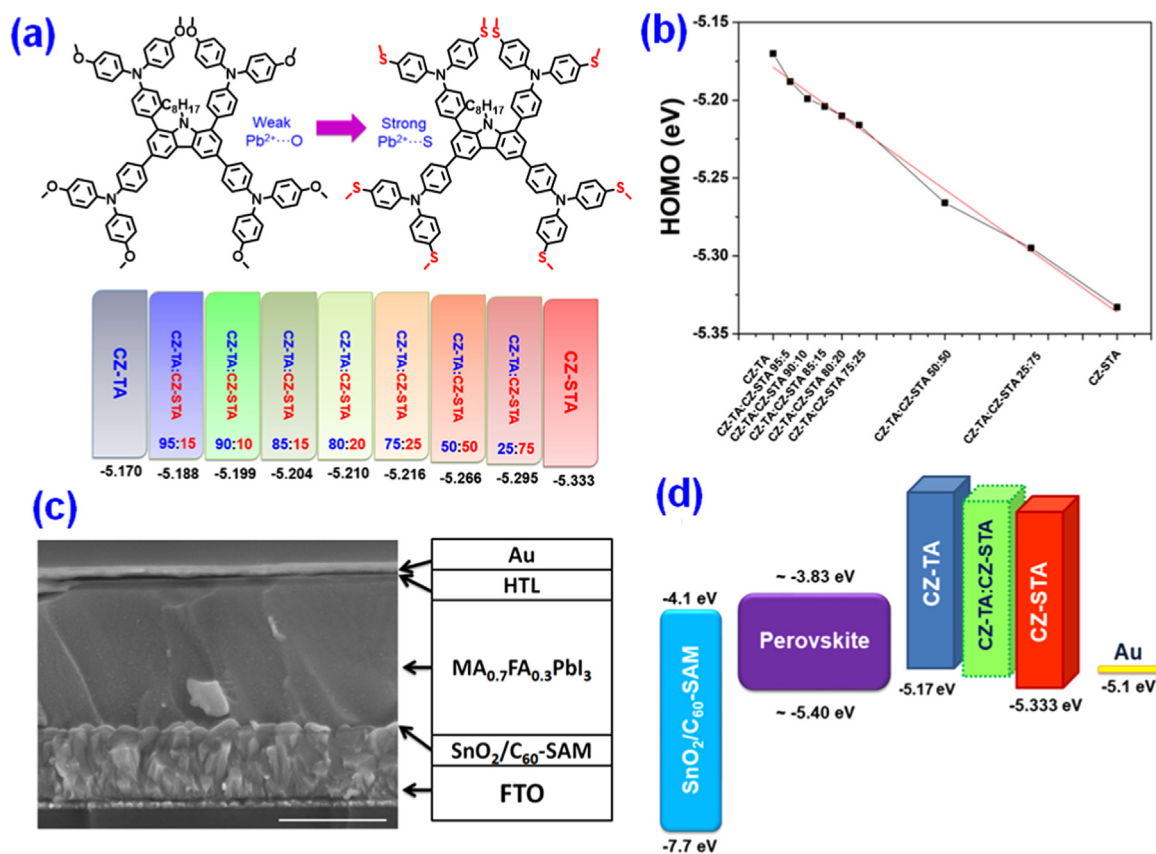
Fig. 2. (a) Chemical structures of CZ-TA and CZ-STA, together with HOMO values of their blends of different compositions in weight ratios. (b) Correlation of binary HTLs' HOMO levels with different CZ-TA:CZ-STA blends. (a) Cross-sectional SEM image of PVSC with CZ-TA:CZ-STA (90:10, w/w) as HSL. The scale bar is 500 nm. (b) Energy level diagram of PVSC.

carefully characterized by nuclear magnetic resonance (NMR) (Fig. S1-S10, ^{1}H, ^{13}C, SI) and matrix-assisted laser desorption ionization/time of flight (MADLI-TOF) mass spectrometry (Fig. S11, SI). Similar to CZ-TA, CZ-STA also showed good solubility in common organic solvents such as toluene, chlorobenzene and chloroform. Besides, CZ-TA and CZ-STA have good miscibility and compatibility due to their similar backbone structure. Thermogravimetric analysis (TGA) indicates that CZ-STA has good thermal stability with 5% weight loss found till 401 °C (Fig. S12a, SI), which is far above temperatures for device fabrication. From differential scanning calorimetry (DSC) result, a glass transition temperature (T_g) at 110.2 °C is observed for CZ-STA (Fig. 12b, SI), indicating its amorphous nature which may help to form uniform and pinhole-free HTL films [21,36].

Fig. 1**b** shows the UV–Vis absorption spectrum of CZ-STA film. The maximum peak is located at 333 nm, with an onset absorption around 400 nm. According to $E_g = 1240/\lambda_{onset}$, the optical bandgap ($E_g$) of CZ-STA can be estimated as 3.10 eV. To evaluate the energy levels of CZ-STA, cyclic voltammetry (CV) was adopted with ferrocene/ferrocenium (Fc/Fc$^+$) as the internal standard. In the inset of Fig. 1**b**, a clear oxidation peak is observed with an onset potential of 0.883 V. The HOMO level of CZ-STA was thus determined to be −5.333 eV. Then, the LUMO level can be accordingly estimated to be −2.233 eV [26], which would efficiently block electrons from recombining with holes. Compared with original CZ-TA, CZ-STA exhibits deeper HOMO level after incorporation of methythiol ending group, CV result agrees well with our DFT

simulation. For CZ-STA, this deep HOMO level may be negative for generating enough driving force for hole transfer since the valence band of MA$_{0.7}$FA$_{0.3}$PbI$_3$ (MA: methylammonium, FA: formamidinium) is around −5.40 eV.[28,37] Opposite for CZ-TA (HOMO = −5.17 eV), a small downshift of HOMO level is required to enhance its photovoltaic performance.

As shown in Fig. 2**a&b**, we obtained a continuously adjustable HOMO level from −5.17 eV to −5.333 eV through simply changing the weight ratios of CZ-TA:CZ-STA blends. HOMO levels were almost linearly decreased along the increase of CZ-STA ratios, suggesting that CZ-TA and CZ-STA form very compatable blends [32,34,38]. To evaluate the device performance of binary HTL with different ratios, we fabricated a large number of PVSCs with the conventional device structure of FTO/SnO$_2$/C$_{60}$-SAM/MA$_{0.7}$FA$_{0.3}$PbI$_3$/CZ-TA:CZ-STA/Au. As clearly shown in Fig. 2**c**, a HTL layer of approximately 50 nm was uniformly deposited onto the top of perovskite. Large grains comparable with the thickness of perovskite layer facilitate the charge transport by reducing grain boundaries and the density of corresponding traps [39,40].

Fig. 3 shows the statistics of V_{OC}, J_{SC}, FF, and PCE of PVSCs using different CZ-TA:CZ-STA blends as HTL. By adjusting the weight ratio of CZ-TA and CZ-STA from 100:0 to 90:10, we observed the average V_{OC} increased from 1.041 V to 1.083 V and J_{SC} reached 22.43 mA cm^{-2} from the initial 21.70 mA cm^{-2} and FF maintained over 80%. However, further increased CZ-STA content (> 10% in weight ratio) led to simultaneous reduced V_{OC}, J_{SC}, and FF, therefore, PCE. The detailed
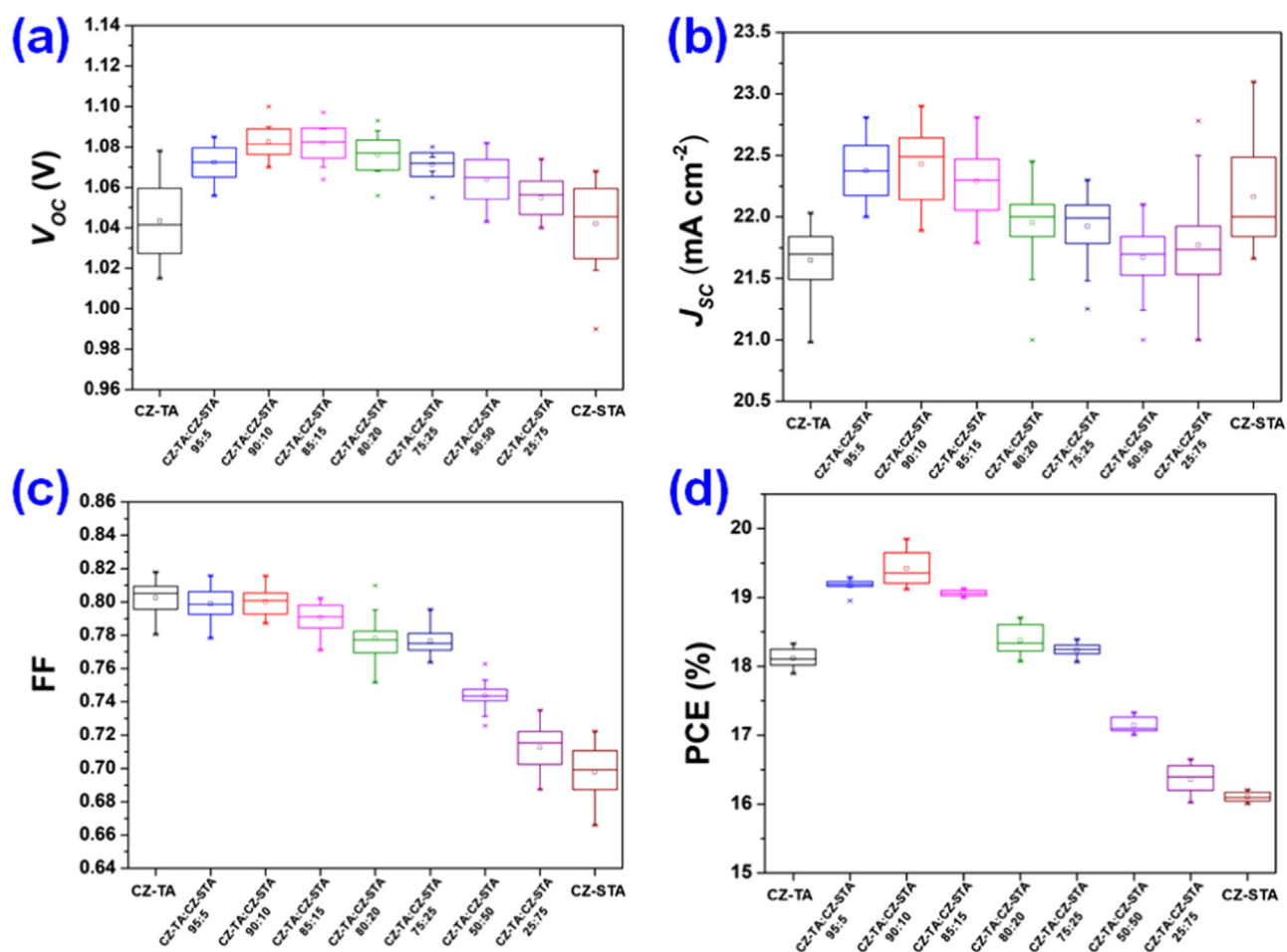
Fig. 3. Photovoltaic parameters of PVSCs with different CZ-TA:CZ-STA ratios. Histograms of (a) V_{OC}, (b) J_{SC}, (c) FF, and (d) PCE of corresponding devices.

parameters of champion PVSCs using different blends as HTL are listed in Table S1. A close look at the HOMO-LUMO energy levels change with blend composition (Table S1), one can found the blend HTL exhibits both decreased HOMO and LUMO energy levels with the increased addition of CZ-STA, resulting in decreased V_{OC} of PVSCs (Fig. 3a). The CZ-TA:CZ-STA (90:10) blend achieves a HOMO of -5.199 eV, matching perfectly with that of Spiro-OMeTAD (-5.20 eV). This best alignment of energy levels facilitates the hole extraction and transport from this binary blend HTL, thus leading to the champion PCE of 19.85%. Further deepening the HOMO levels of binary blend with increased addition of CZ-STA, PVSCs will lose enough driving force for hole-extraction and cause surface recombination, which may result in V_{OC} loss and poor FF. Similar phenomenon has been observed by Polander and their coworkers [41].

Besides for the ideal HOMO achieved at 10% addition of CZ-STA, the binary blends with CZ-STA content > 10 wt% exhibit decreased compatibility and thus clearer phase separation between two components on top of perovskite with the increased addition of CZ-STA (evidence shown by AFM images in Fig. 6). The less compatibility of binary HTL blends will result in enhanced hole traps and poorer Ohmic contact at the interfaces with perovskite, reflecting by the decreased J_{SC} and FF values for PVSCs (Fig. 3b &c). As a whole, PVSCs with binary blend HTLs containing no more than 25 wt% CZ-STA contribute higher

PCEs than corresponding devices with individual component HTLs (Fig. 3d).

Fig. 4**a** shows the *J-V* curve under reverse and forward voltage scan of our best-performing PVSCs with CZ-TA, CZ-STA or CZ-TA:CZ-STA blends as HTLs under 100 mW/cm^2 AM1.5G illumination. The PVSC employing only CZ-TA (CZ-STA) as HTL shows a relatively low PCE of 18.32% (16.21%) with a J_{SC} of 21.66 (21.96) mA cm^{-2}, a V_{OC} of 1.044 (1.052) V, and a FF of 0.810 (0.702) under reverse scan. The low V_{OC} and J_{SC} of pristine CZ-TA along with the low V_{OC} and FF of pristine CZ-STA can be attributed to energy loss resulting from energy-level mismatch.

When CZ-STA was blended into CZ-TA, the PVSC showed a significantly increased PCE with the simultaneously improved J_{SC}, V_{OC}, and high FF values. The HTL with CZ-TA:CZ-STA (90:10) blend for PVSCs affords a champion PCE of 19.85%, with a J_{SC} of 22.51 mA cm^{-2}, a V_{OC} of 1.082 V, and a FF of 0.815. Compared to the large hysteresis ($\sim$ 2% PCE hysteresis) of using CZ-TA only as HTL, the binary CZ-TA:CZ-STA (90:10) based PVSCs exhibited negligible hysteresis. This could be explained by the passivation effect at HTL-perovskite interface due to interaction between Pb^{2+} and S.[31] The integrated J_{sc} of PVSCs with CZ-TA or CZ-TA:CZ-STA (90:10) HTL from EQE is 21.39 mA cm^{-2} and 22.46 mA cm^{-2}, which are consistent with *J-V* results. Additionally, the steady-state output photocurrent of CZ-
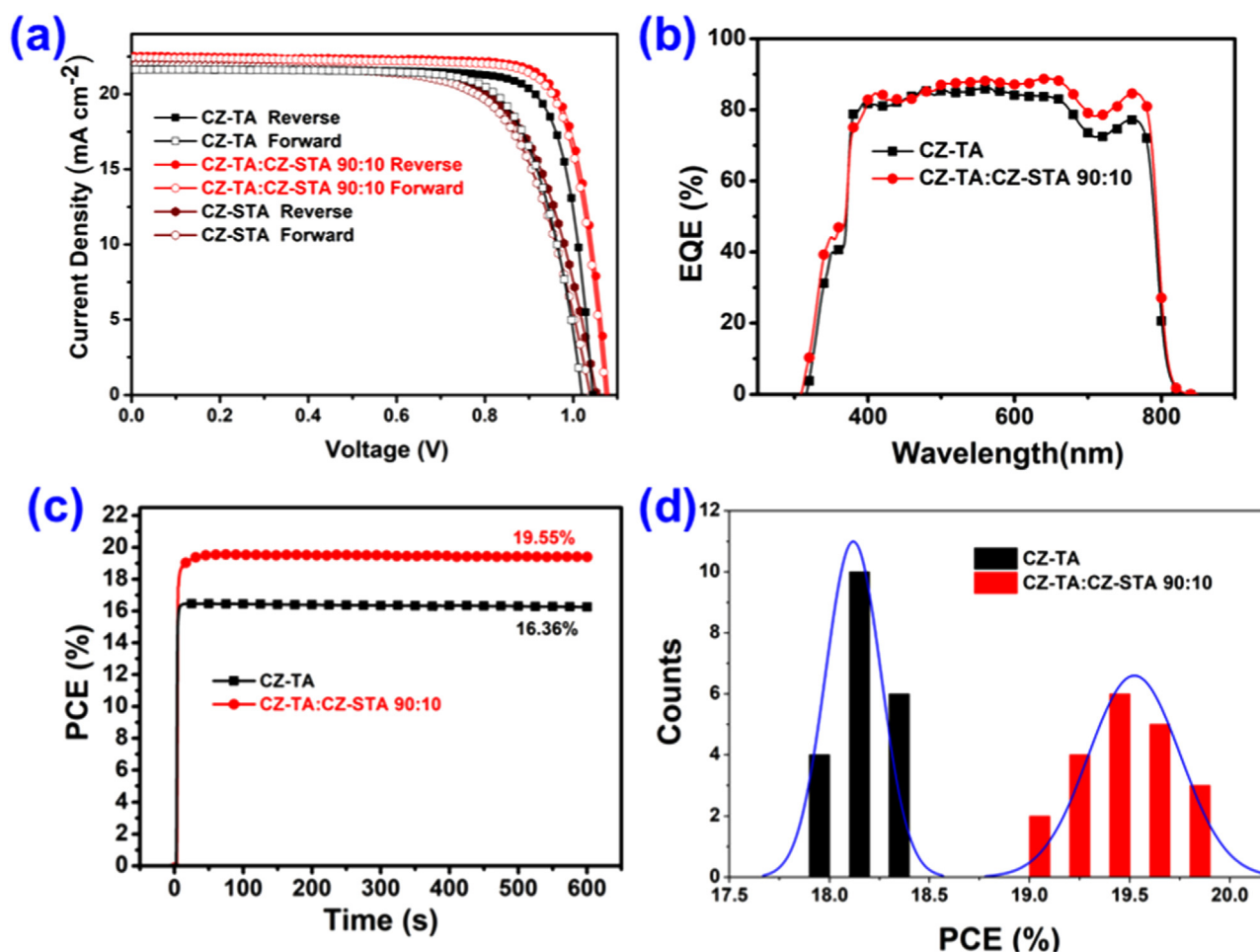
Fig. 4. (a) *J-V* curve under 100 mW/cm² AM1.5G illumination of PVSCs with CZ-TA and CZ-TA:CZ-STA (90:10) HTL, (b) EQE spectra of best-performing PVSCs with CZ-TA or CZ-TA:CZ-STA (90:10) HTL. (c) Steady-state efficiency of our best-performing PVSC with CZTA or CZ-TA:CZ-STA (90:10) HTL. (d) Histogram of PCEs measured for 20 cells using CZ-TA or CZ-TA:CZ-STA (90:10) HTL.

TA:CZ-STA (90:10) HTL based devices at a constant applied voltage of 0.920 V for 600 s is around 21.27 mA cm^{-2}, leading to a stabilized PCE of ~ 19.55%. As shown in Fig. 4d, the average PCE of 19.42 ± 0.43% with an average V_{OC} of 1.083 ± 0.017 V, an average J_{SC} of 22.43 ± 0.47 mA cm^{-2}, and an average FF of 0.800 ± 0.015 for devices using CZ-TA:CZ-STA (90:10) blend as HTL are obtained from 20 cells fabricated in different batches.

Fig. 5a shows the steady-state photoluminescence (PL) spectra of perovskite films with or without HTL layers on top. By adding HTL layer onto the surface of perovskite film, strong PL quenching is observed. HTLs with CZ-STA content smaller than 15 wt% shows a higher quenching efficiency than pristine CZ-TA, indicating that the stronger interaction between sulfur and Pb^{2+} as well as more suitable band alignment benefits better hole extract and transfer from perovskite to HTL. It is worth noting that CZ-TA:CZ-STA (90:10) quenches most effectively among all blends, agreeing well with its superior device performance. The TRPL decays are shown in Fig. 5b. With the deposition of HTL layer onto perovskite film, the mean carrier lifetime is greatly shortened from 1200 ns to 191 ns and 278 ns for CZ-TA and CZ-STA, respectively. The shortest lifetime is obtained from CZ-TA:CZ-STA

90:10 again, indicating its most efficient dissociation and fastest charge transfer. This may also contribute to reduced recombination and enhanced J_{SC}.

To further understand the recombination mechanism in these PVSCs, we further investigated the dependence of J and V characteristics on light intensity from 1 to 100 mW/cm². Fig. 5c shows the dependence of J_{SC} on light intensity ($J \propto I^{\alpha}$) by power law. It is known that an α value closes to 1 indicates no space charge effect exists in a solar cell, while an α value of 0.75 implies large space charge effect due to interfacial barrier or charge imbalance [26,42,43]. Therefore, when increasing CZ-STA weight ratio in CZ-TA:CZ-STA binary HTLs, the PVSCs appear to be more space charge limited, especially for CZ-TA:CZ-STA (25:75) based devices. Fig. 5d shows V_{OC} varies logarithmically with light intensity. In principle, the slope will be equal to 2 kT/e if the monomolecular recombination (Shockley–Read–Hall recombination) is dominant, while the slope will be equal to 1 kT/e if bimolecular recombination governs. For pure CZ-TA and CZ-TA:CZ-STA (90:10) HTLs, less Shockley–Read–Hall recombinations are observed. These results suggest that CZ-TA blending with 10 wt% CZ-STA can not only more efficiently extract the holes but also reduce recombination
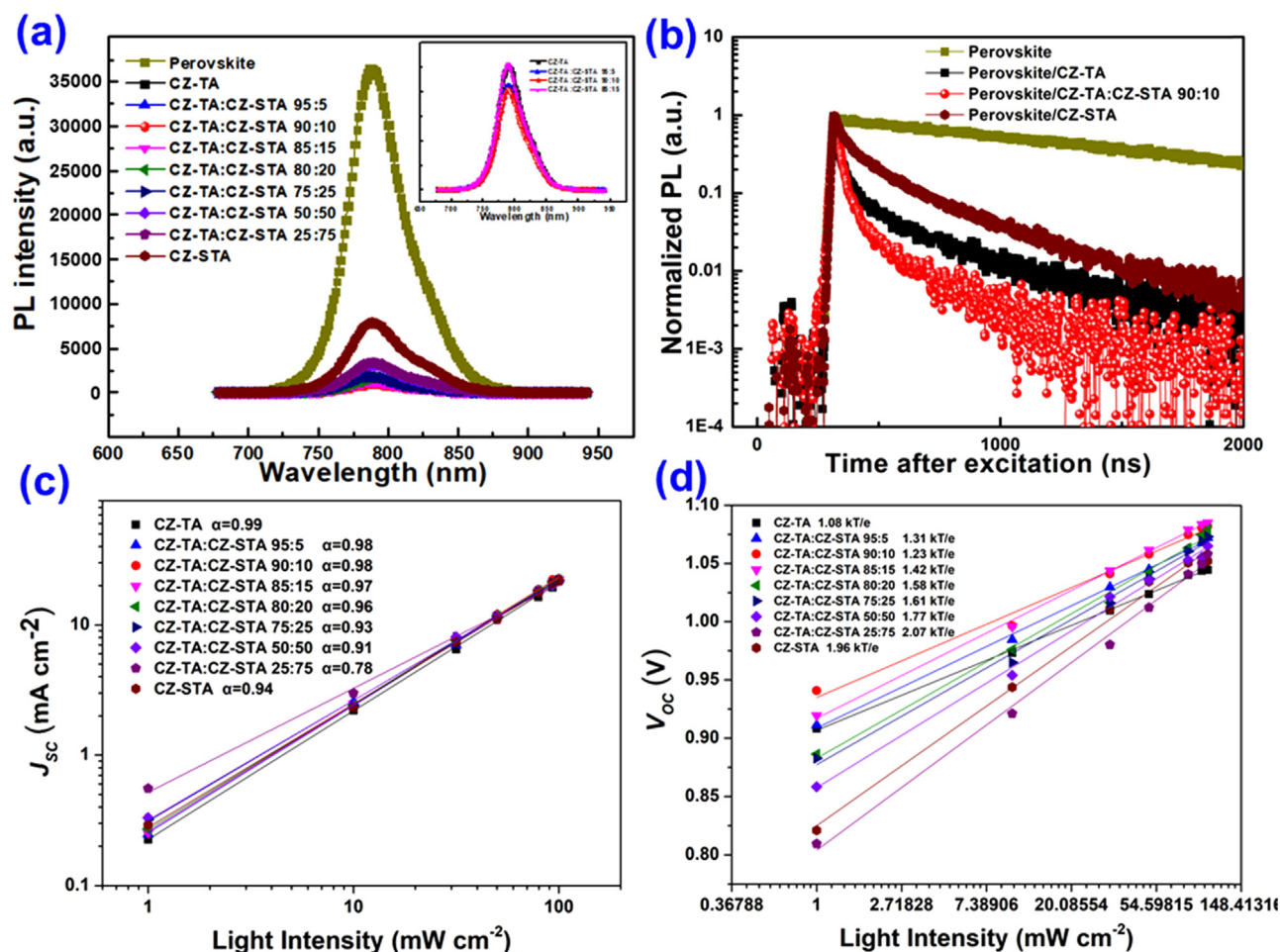
Fig. 5. (a) PL intensity of perovskite film and perovskite/HTL, the inset is perovskite film/CZ-TA:CZ-STA blend with composition varied from 100:0 to 85:15. (b) TRPL decays of perovskite film and perovskite films with CZ-TA, CZ-TA:CZ-STA 90:10 or CZ-STA as HTLs. Influence of light intensity on (c) J_{sc} and (d) V_{oc} of PVSCs with CZ-TA, CZ-STA or their blends with different weight ratios as HTLs.

In order to investigate the charge transport behavior, the hole mobilities of CZ-TA and all CZ-TA:CZ-STA blends were measured by the method of space-charge-limited current (SCLC). It is clear in Fig. 6a that both CZ-TA (2.40×10^{-4} cm^2 V^{-1} s^{-1}) and CZ-TA:CZ-STA blends (no less than 2×10^{-4} cm^2 V^{-1} s^{-1}) have much higher mobility than Spiro-OMeTAD (1.11×10^{-5} cm^2 V^{-1} s^{-1}). The morphology of blended HTL film was characterized by atomic force microscopy (AFM) in tapping mode. As shown in Fig. 6b, no obvious phase separation or aggregation was observed until CZ-STA reached 50 wt%, indicating good compatibility of CZ-TA and CZ-STA.

To check the device stability with binary HTLs, we compared the environmental stability of PVSCs using CZ-TA:CZ-STA (90:10) blend and doped spiro-OMeTAD as HTLs without encapsulation in ambient air under a relative humidity of ~50%. The PCE decay curves are presented in Fig. 6c, CZ-TA:CZ-STA (90:10) HTL based device shows much improved ambient stability, indicating by 82% of initial PCE retained after 60 days. On the contrary, the spiro-OMeTAD-based device lost almost 90% of its PCE within the same time window. Thus, our binary CZ-TA:CZ-STA (90:10) HTL not only delivers a high PCE, but also an

enhanced device stability, making it promising candidate for pushing forward the development of perovskite solar cells.

3. Conclusions

In summary, we have developed a binary HTL blend strategy for facilely and continuously tuning the HOMO level of HTL to realize significantly enhanced photovoltaic performance and device stability for PVSCs. By adding 10 wt% methylthio-substituted CZ-STA to CZ-TA as blend HTL, we successfully improved the V_{OC} from 1.044 V to 1.083 V due to optimized energy-level alignment. Moreover, better charge extraction and interface passivation resulting from strong Pb^{2+}-S interaction led to enhanced J_{SC} and reduced hysteresis with a remarkable FF of 0.815. Planar PVSCs using CZ-TA:CZ-STA (90:10) HTL achieved a maximum PCE of 19.85% under reverse voltage scan and a steady-state efficiency of 19.55%. More importantly, the CZ-TA:CZ-STA (90:10) based devices retained over 82% of its initial PCE after storing for 60 days in air with a relative humidity around 50% without encapsulation, revealing the great potential for improving long-term
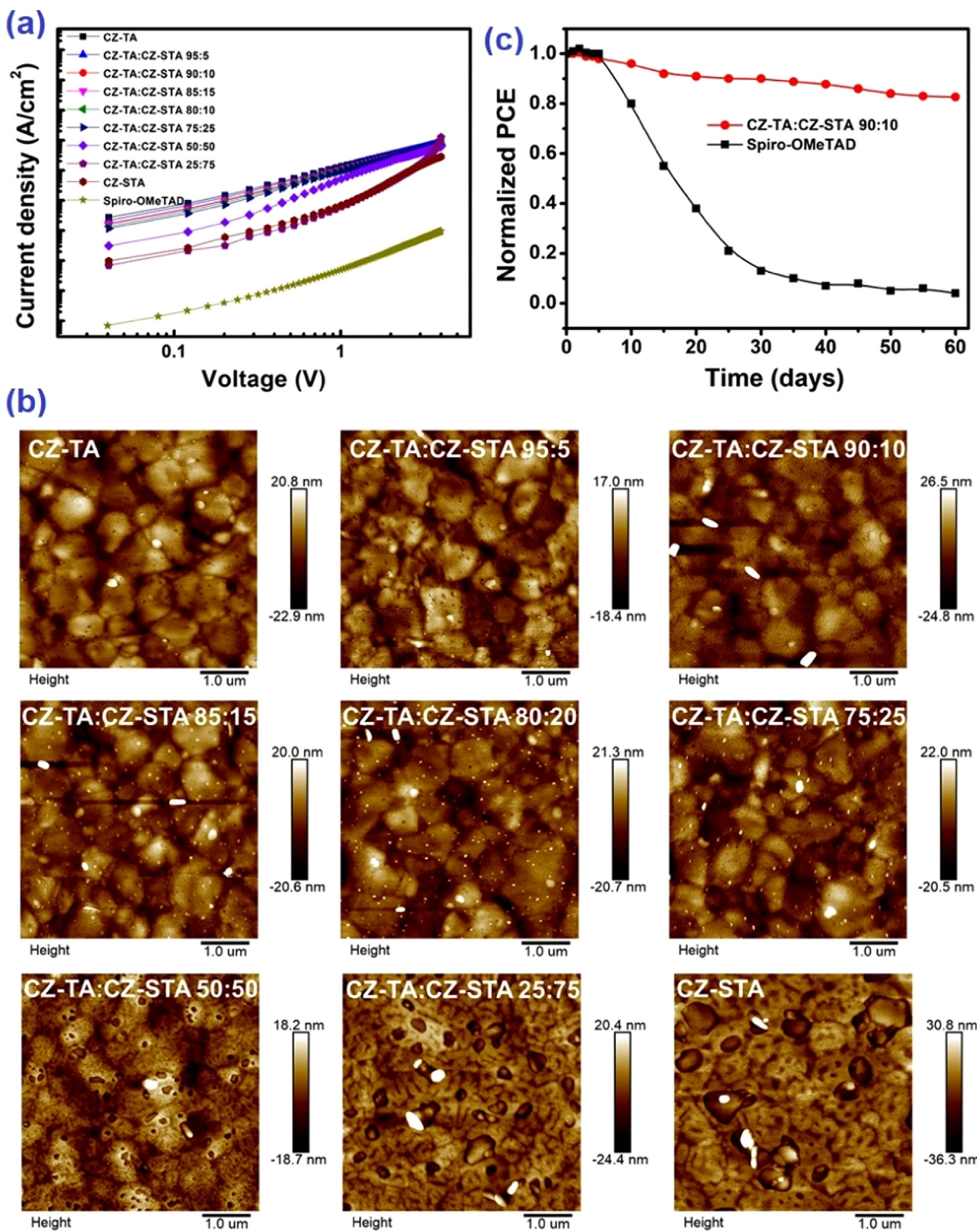
Fig. 6. (a) Space-charge-limited current (SCLC) *J–V* characteristics of CZ-TA:CZ-STA-based hole-only devices. (b) AFM images (5 μm × 5 μm) of perovskite/HTLs. (c) The stability test of the conventional PVSCs in ambient air with a humidity of ~ 50%.

device stability. Therefore, our work brings a new sight for developing hole transport materials to achieve high-efficiency stable perovskite solar cells.

Acknowledgements

Appendix A. Supporting information

Supplementary data associated with this article can be found in the online version at doi:10.1016/j.nanoen.2018.07.027.

References

[1] W.-J. Yin, T. Shi, Y. Yan, Adv. Mater. 26 (2014) 4653–4658.
[2] W. Nie, H. Tsai, R. Asadpour, J.-C. Blancon, A.J. Neukirch, G. Gupta, J.J. Crochet, M. Chhowalla, S. Tretiak, M.A. Alam, H.-L. Wang, A.D. Mohite, Science 347 (2015) 522–525.
[3] S.D. Stranks, G.E. Eperon, G. Grancini, C. Menelaou, M.J.P. Alcocer, T. Leijtens, L.M. Herz, A. Petrozza, H.J. Snaith, Science 342 (2013) 341–344.
[4] M.A. Green, A. Ho-Baillie, H.J. Snaith, Nat. Photon. 8 (2014) 506–514.
[5] Y.-M. You, W.-Q. Liao, D. Zhao, H.-Y. Ye, Y. Zhang, Q. Zhou, X. Niu, J. Wang, P.-F. Li, D.-W. Fu, Z. Wang, S. Gao, K. Yang, J.-M. Liu, J. Li, Y. Yan, R.-G. Xiong, Science 357 (2017) 306–309.
[6] A. Kojima, K. Teshima, Y. Shirai, T. Miyasaka, J. Am. Chem. Soc. 131 (2009) 6050–6051.
[7] D.P. McMeekin, G. Sadoughi, W. Rehman, G.E. Eperon, M. Saliba, M.T. Hörantner, A. Haghighirad, N. Sakai, L. Korte, B. Rech, M.B. Johnston, L.M. Herz, H.J. Snaith, Science 351 (2016) 151–155.
[8] S.S. Shin, E.J. Yeom, W.S. Yang, S. Hur, M.G. Kim, J. Im, J. Seo, J.H. Noh, S.I. Seok, Science 356 (2017) 167–171.
[9] Y. Hou, X. Du, S. Scheiner, D.P. McMeekin, Z. Wang, N. Li, M.S. Killian, H. Chen, M. Richter, I. Levchuk, Science 358 (2017) 1192–1197.
[10] W.S. Yang, B.-W. Park, E.H. Jung, N.J. Jeon, Y.C. Kim, D.U. Lee, S.S. Shin, J. Seo, E.K. Kim, J.H. Noh, S.I. Seok, Science 356 (2017) 1376–1379.
[11] J.-P. Correa-Baena, A. Abate, M. Saliba, W. Tress, T. Jesper Jacobsson, M. Grätzel, A. Hagfeldt, Energy Environ. Sci. 10 (2017) 710–727.
[12] P. Agarwala, D. Kabra, J. Mater. Chem. A 5 (2017) 1348–1373.
[13] A. Krishna, A.C. Grimsdale, J. Mater. Chem. A 5 (2017) 16446–16466.
[14] M.L. Petrus, J. Schlipf, C. Li, T.P. Gujar, N. Giesbrecht, P. Müller-Buschbaum, M. Thelakkat, T. Bein, S. Hüttner, P. Docampo, Adv. Energy Mater. 7 (2017) 1700264.
[15] M. Saliba, T. Matsui, K. Domanski, J.-Y. Seo, A. Ummadisingu, S.M. Zakeeruddin, J.-P. Correa-Baena, W.R. Tress, A. Abate, A. Hagfeldt, M. Grätzel, Science 354 (2016) 206–209.
[16] Q. Jiang, Z. Chu, P. Wang, X. Yang, H. Liu, Y. Wang, Z. Yin, J. Wu, X. Zhang, J. You, Adv. Mater. 29 (2017) 1703852.
[17] T. Bu, X. Liu, Y. Zhou, J. Yi, X. Huang, L. Luo, J. Xiao, Z. Ku, Y. Peng, F. Huang, Y.-B. Cheng, J. Zhong, Energy Environ. Sci. 10 (2017) 2509–2515.
[18] M. Li, Z.K. Wang, M.P. Zhuo, Y. Hu, K.H. Hu, Q.Q. Ye, S.M. Jain, Y.G. Yang, X.Y. Gao, L.S. Liao, Adv. Mater. (2018) 1800258.
[19] C. Rodríguez-Seco, L. Cabau, A. Vidal-Ferran, E. Palomares, Acc. Chem. Res. 51 (2018) 869–880.
[20] K. Gao, Z. Zhu, B. Xu, S.B. Jo, Y. Kan, X. Peng, A.K.Y. Jen, Adv. Mater. 29 (2017) 1703980.
[21] T. Malinauskas, M. Saliba, T. Matsui, M. Daskeviciene, S. Urnikaite, P. Gratia, R. Send, H. Wonneberger, I. Bruder, M. Grätzel, V. Getautis, M.K. Nazeeruddin, Energy Environ. Sci. 9 (2016) 1681–1686.
[22] N. Arora, M.I. Dar, A. Hinderhofer, N. Pellet, F. Schreiber, S.M. Zakeeruddin, M. Grätzel, Science 358 (2017) 768–771.
[23] L. Guan, X. Yin, D. Zhao, C. Wang, Q. An, J. Yu, N. Shrestha, C. Grice, R. Awni, Y. Yu, Z. Song, J. Zhou, W. Meng, F. Zhang, R. Ellingson, J. Wang, W. Tang, Y. Yan, J. Mater. Chem. A 5 (2017) 23319–23327.
[24] Y. Sun, C. Wang, D. Zhao, J. Yu, X. Yin, C.R. Grice, R.A. Awni, N. Shrestha, Y. Yu, L. Guan, R.J. Ellingson, W. Tang, Y. Yan, Sol. RRL 2 (2018) 1700175.
[25] M. Saliba, S. Orlandi, T. Matsui, S. Aghazada, M. Cavazzini, J.-P. Correa-Baena, P. Gao, R. Scopelliti, E. Mosconi, K.-H. Dahmen, F. De Angelis, A. Abate, A. Hagfeldt, G. Pozzi, M. Graetzel, M.K. Nazeeruddin, Nat. Energy 1 (2016) 15017.
[26] X. Yin, L. Guan, J. Yu, D. Zhao, C. Wang, N. Shrestha, Y. Han, Q. An, J. Zhou, B. Zhou, Y. Yu, C.R. Grice, R.A. Awni, F. Zhang, J. Wang, R.J. Ellingson, Y. Yan, W. Tang, Nano Energy 40 (2017) 163–169.
[27] D.-B. Li, X. Yin, C.R. Grice, L. Guan, Z. Song, C. Wang, C. Chen, K. Li, A.J. Cimaroli, R.A. Awni, D. Zhao, H. Song, W. Tang, Y. Yan, J. Tang, Nano Energy 49 (2018) 346–353.
[28] Y. Bai, X. Meng, S. Yang, Adv. Energy Mater. 8 (2018) 1701883.
[29] X. Yin, Q. An, J. Yu, Z. Xu, P. Deng, Y. Geng, B. Zhou, F. Zhang, W. Tang, Dyes Pigment. 140 (2017) 512–519.
[30] C. Cui, W.-Y. Wong, Y. Li, Energy Environ. Sci. 7 (2014) 2276–2284.
[31] H. Chen, W. Fu, C. Huang, Z. Zhang, S. Li, F. Ding, M. Shi, C.-Z. Li, A.K.Y. Jen, H. Chen, Adv. Energy Mater. 7 (2017) 1700012.
[32] Q. An, F. Zhang, X. Yin, Q. Sun, M. Zhang, J. Zhang, W. Tang, Z. Deng, Nano Energy 30 (2016) 276–282.
[33] Q. An, F. Zhang, Q. Sun, M. Zhang, J. Zhang, W. Tang, X. Yin, Z. Deng, Nano Energy 26 (2016) 180–191.
[34] T.L. Nguyen, H. Choi, S.-J. Ko, M.A. Uddin, B. Walker, S. Yum, J.-E. Jeong, M.H. Yun, T.J. Shin, S. Hwang, J.Y. Kim, H.Y. Woo, Energy Environ. Sci. 7 (2014) 3040–3051.
[35] M. Planells, A. Abate, D.J. Hollman, S.D. Stranks, V. Bharti, J. Gaur, D. Mohanty, S. Chand, H.J. Snaith, N. Robertson, J. Mater. Chem. A 1 (2013) 6949–6960.
[36] F. Zhang, Z. Wang, H. Zhu, N. Pellet, J. Luo, C. Yi, X. Liu, H. Liu, S. Wang, X. Li, Y. Xiao, S.M. Zakeeruddin, D. Bi, M. Grätzel, Nano Energy 41 (2017) 469–475.
[37] W. Zhou, Z. Wen, P. Gao, Adv. Energy Mater. 8 (2018) 1702512.
[38] R. Yu, H. Yao, J. Hou, Adv. Energy Mater. (2018) 1702814.
[39] C. Wang, C. Xiao, Y. Yu, D. Zhao, R.A. Awni, C.R. Grice, K. Ghimire, D. Constantinou, W. Liao, A.J. Cimaroli, P. Liu, J. Chen, N.J. Podraza, C.-S. Jiang, M.M. Al-Jassim, X. Zhao, Y. Yan, Adv. Energy Mater. 7 (2017) 1700414.
[40] D. Zhao, Y. Yu, C. Wang, W. Liao, N. Shrestha, C.R. Grice, A.J. Cimaroli, L. Guan, R.J. Ellingson, K. Zhu, X. Zhao, R.-G. Xiong, Y. Yan, Nat. Energy 2 (2017) 17018.
[41] L.E. Polander, P. Pahner, M. Schwarze, M. Saalfrank, C. Koerner, K. Leo, APL Mater. 2 (2014) 081503.
[42] D. Zhao, M. Sexton, H.-Y. Park, G. Baure, J.C. Nino, F. So, Adv. Energy Mater. 5 (2015) 1401855.
[43] C. Wang, D. Zhao, Y. Yu, N. Shrestha, C.R. Grice, W. Liao, A.J. Cimaroli, J. Chen, R.J. Ellingson, X. Zhao, Y. Yan, Nano Energy 35 (2017) 223–232.